Flight Times to the Heliopause Using a Combination of Solar and Radioisotope Electric Propulsion

IEPC-2011-051

Presented at the 32nd International Electric Propulsion Conference,
Wiesbaden, Germany
September 11–15, 2011

Andreas Ohndorf*
German Aerospace Center (DLR), P.O. 1116, Wessling, 82230, Germany

Bernd Dachwald†
FH University of Applied Sciences, Hohenstaufenallee 6, Aachen, 52064, Germany

Wolfgang Seboldt‡
German Aerospace Center (DLR), Linder Hoehe, Cologne, 51147, Germany

and

Horst W. Loeb and Karl-Heinz Schartner§
University of Giessen, Heinrich Buff Ring 16, Giessen, 35392, Germany

We investigate the interplanetary flight of a low-thrust space probe to the heliopause, located at a distance of about 200 AU from the Sun. Our goal was to reach this distance within the 25 years postulated by ESA for such a mission (which is less ambitious than the 15-year goal set by NASA). Contrary to solar sail concepts and combinations of ballistic and electrically propelled flight legs, we have investigated whether the set flight time limit could also be kept with a combination of solar-electric propulsion and a second, RTG-powered upper stage. The used ion engine type was the RIT-22 for the first stage and the RIT-10 for the second stage. Trajectory optimization was carried out with the low-thrust optimization program *InTrance*, which implements the method of Evolutionary Neurocontrol, using Artificial Neural Networks for spacecraft steering and Evolutionary Algorithms to optimize the Neural Networks' parameter set. Based on a parameter space study, in which the number of thrust units, the unit's specific impulse, and the relative size of the solar power generator were varied, we have chosen one configuration as reference. The transfer time of this reference configuration was 29.6 years and the fastest one, which is technically more challenging, still required 28.3 years. As all flight times of this parameter study were longer than 25 years, we further shortened the transfer time by applying a launcher-provided hyperbolic excess energy up to 49 km^2/s^2. The resulting minimal flight time for the reference configuration was then 27.8 years. The following, more precise optimization to a launch with the European Ariane 5 ECA rocket reduced the transfer time to 27.5 years. This is the fastest mission design of our study that is flexible enough to allow a launch every year. The inclusion of a fly-by at Jupiter finally resulted in a flight time of 23.8 years, which is below the set transfer-time limit. However, compared to the 27.5-year transfer, this mission design has a significantly reduced launch window and mission flexibility if the escape direction is restricted to the heliosphere's "nose".

*Project Manager, Space Operations and Astronaut Training, andreas.ohndorf@dlr.de
†Professor, Aerospace Engineering, dachwald@fh-aachen.de
‡Senior Scientist, Institute of Space Systems, wolfgang.seboldt@dlr.de.
§Professor, 1st Institute of Physics, {horst.w.loeb|karl-heinz.schartner}@exp1.physik.uni-giessen.de

Nomenclature

AU	= astronomical unit, mean Earth-Sun distance (1 AU = 149 597 870 697 m)
C_3	= hyperbolic excess energy
d	= Gravity Assist (GA) fly-by distance
J	= cost function, fitness
m_0	= launch mass
m_p	= propellant mass
n	= number of ion thrusters
P_c	= solar power generator electrical power output at 1 AU distance from the Sun; fraction of P_m
P_m	= maximum electrical power of the SEP stage
v_∞	= hyperbolic excess velocity
I_{sp}	= specific impulse
r	= distance
R_J	= Jupiter radius
U_+	= acceleration grid voltage
t	= (modified Julian) date (MJD)
Δt	= transfer duration
Δv	= velocity increment
w_{ij}	= connection weight between neuron i and neuron j
y_i	= output value of neuron i
γ	= fit parameter
γ_i	= temperature parameter of neuron i
$\boldsymbol{\pi}$	= network parameter vector
θ_i	= threshold value of neuron i

I. Introduction

The outer regions of the heliosphere, where the solar wind encounters the local interstellar medium at a distance of approximately 200 astronomical units (AU), are of scientific interest for decades[1]. We do not know if our models of the processes in that intermediate region are correct and therefore need to test the underlying theories with direct measurements. The problem that inhibits us from making these measurements is the vast distance of 200 AU. No spacecraft has yet traveled that far, and, according to current mission planning*, even the deep space probes Voyager 1 and 2 are uncertain to be still able to return scientific data when they have reached 130 – 140 AU, which will be 2015 for Voyager 1.

ESA and NASA have therefore both included such an Interstellar Heliopause Probe (IHP) mission into their strategic programs. The maximum allowed mission duration is 25 years for ESA missions and 15 years for NASA missions, which corresponds to average velocities of 8 AU/yr and 13.3 AU/yr, respectively. Such average flight velocities and the resulting total velocity increments (Δv) pose a challenging requirement to current propulsion systems. In fact, the unavailability of mature propulsion systems having the required performance characteristics is the main reason why such a mission has not yet been undertaken.

A promising propulsion concept that enables a large Δv is solar sailing. It has been used for past IHP mission studies[2,3], and also radioisotope power generation with electric propulsion in combination with hyperbolic excess energy and gravity assist maneuvers were investigated[4]. Solar sailing, however, is still far from practical big-scale realization. Therefore we investigated a different, technically more mature, propulsion concept and supported our concept with trajectory optimization runs carried out with the program *InTrance*. This program can optimize low-thrust trajectories by making use of Artificial Neural Networks (ANN) and Evolutionary Algorithms (EA) in a method called Evolutionary Neurocontrol (ENC). Our concept consists of the IHP science probe, which is propelled by a solar-electric propulsion (SEP) stage with RIT-22-type thrust

*http://voyager.jpl.nasa.gov/spacecraft/spacecraftlife.html

modules. Additionally, a second upper stage accelerates – after jettison of the SEP-stage – the probe with smaller RIT-10-engines that are powered by four radioisotope thermal generators (RTG). We started with a variation of the solar power generator characteristic power P_c, the number of thrust modules n, and the thrust modules acceleration grid voltage U_+ and therefore its specific impulse, I_{sp}, to determine the transfer time's sensitivity to these parameters. These optimization runs were conducted with hyperbolic excess energy (relative to Earth) $C_3 = 0$ for 27 SEP-only and for 27 SEP+REP configurations. The resulting transfer times were still above the 25-year limit and then we included the potential launcher-provided hyperbolic excess energy for interplanetary injection, e.g., by an Ariane 5 ECA, which reduced the flight time further, but still being above 25 years. Finally, we included a gravity assist at Jupiter which resulted in a transfer time of only 23.4 years.

II. Low-Thrust Trajectory Optimization with *InTrance*

For the trajectory calculations within this work we used the low-thrust trajectory optimization software *InTrance*, which stands for "*In*telligent *Tra*jectory optimization using *n*euro*c*ontroller *e*volution", developed by two of us (B. Dachwald and A. Ohndorf). It is an implementation of the *Evolutionary Neurocontrol* (ENC) method - a combination of *Artificial Neural Networks* (ANN) and *Evolutionary Algorithms* (EA). The ANN is used to steer a low-thrust spacecraft (nearly) globally optimal, whereas the EA is used to train the ANN for this specific optimal control task. Both concepts are only briefly described in the next three subsections, but more detailed descriptions can be found in Refs. 5-7. The final subsection briefly deals with the spacecraft configurations that we used for the presented trajectory results. However, as the design and its design-driving requirements are treated extensively in Ref. 8, only the parameters that are relevant for the trajectory calculations are introduced.

A. Artificial Neural Networks

ANNs are the result of the attempt to make use of advantageous features of the biological brain, e.g. information storage and processing, fault tolerance, generalization, and decision making. Like their biological prototype, ANNs basically comprise simple processing units, the *neurons*, and multiple connections between them, i.e. one neuron receives information from at least one other neuron, and provides its own output to other neurons. The output is determined by the sum of all input information and the *transfer function* or *activation function*, which is inherent to each neuron. The respective transfer function can be simple, e.g. a step or a linear function, but throughout this study we have used the commonly used sigmoid transfer function. For every neuron i, the output y_i is calculated from the output y_j of all input neurons j via

$$y_i = \frac{1}{1 + e^{-\left(\sum_j w_{ij} y_j - \theta_i\right)/\gamma_i}}, \tag{1}$$

with the connection weights w_{ij} between neuron i and all input neurons j, the threshold value or bias θ_i of neuron i, and the temperature parameter γ_i of neuron i. An advantage of the sigmoid is its ability to mimic the step function and linear functions, by adjusting the temperature parameter, while still being steady and limiting the output to a minimal and maximal value.

A single neuron's capabilities are limited to its transfer function, but through the interconnection of more than one neuron complex transfer functions become achievable. The only approximately 100 000 cells of a fly brain, for example, enable the fly not only to sense its environment, to find food, and to reproduce, but also to manage the challenging flight control system. The key to success is the optimized transfer behavior of the fly's neurons and their interconnectivity. Using sigmoid-type neurons, the ANN's degree of optimality is then determined by the parameters w_{ij}, θ_i, and γ_i of all neurons i. If organized in a parameter vector $\boldsymbol{\pi} = (\pi_1, \ldots, \pi_k, \ldots, \pi_m)$, where the π_k are the ANN parameters (w_{ij}, θ_i, and γ_i), this m-dimensional vector completely defines the so-called *network function* $\mathbf{N}_\pi$.

For this study we have used ANNs whose internal neurons are organized in layers: the input layer receiving the problem-dependent information (the environment), the output layer giving the network function's result (the control), and eventually existing so-called hidden layers between them. Feed-forward connections transport information between two consecutive layers and thus make data propagation though the ANN deterministic. This type of ANN is called layered feed-forward ANN and has been successfully applied to a number of classification and control problems.

B. Evolutionary Algorithms

Natural evolution provides the enabling principles of evolutionary computer paradigms, one of which being the Evolutionary Algorithm or Genetic Algorithm. This type of global optimization method has been successfully used to solve a number of very different problems and in the following the essential elements of EAs are briefly described whereas the explanation is constrained on how these elements are implemented in *InTrance*. Many of the explained general elements do also exist in different implementations but were not used for this study. These elements are again derived from natural evolution and are therefore the *population* and the mechanisms of *selection*, *crossover*, *mutation*, and *evaluation*.

A core element of EAs is the population, which is a collection of potential solutions to the problem. Using biologic terms, these solution candidates are also called individuals, or chromosomes, or strings ξ. Each individual incorporates exactly one potential solution of the given problem. At the beginning of the algorithm, however, when all individuals are initialized with more or less random content, every solution is far from solving the problem at all or being optimal. If a population member solves the problem at all and, if that is the case, how good it solves the problem, is measured with a single scalar value. It is called objective value, cost function, fitness value, or only the fitness J. With this performance metric all population members are now comparable w.r.t. suitability to solve the problem. The higher the fitness the better an individual solves the given problem.

The second EA element is selection. *InTrance* uses tournament selection and randomly selects four individuals and pairwise compares their fitness values to determine two "winner" and two "looser" individuals. The winners are allowed to reproduce and create offspring individuals. The inferior solutions are replaced by the new offspring solutions and therefore become extincted.

Crossover, the third algorithm element, takes place after selection. The "winner" individuals' genome information is used to form two new individuals. These newborn solution candidates therefore contain genome information of both parents. A simple method is *uniform* crossover, during which genome information is alternately taken from "winner" solution one and "winner" individual two.

The next algorithm element, the mutation, is applied after crossover and introduces a small random change to the value at an also randomly chosen position of the genome code. It helps to to explore the solution space more thoroughly and less dependently on only the population's total genome code.

The final element is the evaluation. It is the problem-dependent element of an EA and assigns the necessary fitness to the newborn population members after mutation. Evaluation is the last algorithm step and a new cycle can start with selection.

The enabling principle of EA is the concept of survival of the fittest. The individual that is adapted best to its current environment has the highest chance to reproduce and therefore to contribute its genome code to the population genome information. With continuing algorithm runtime, the population members' genomes more and more resemble each other and the divergence among their fitness values decreases. At the same time, the population's maximum fitness will increase until no more improvement is achievable. Depending on set convergence criteria, *InTrance* then either stops or initializes a new population based on the former best solution.

C. Evolutionary Neurocontrol for spacecraft steering

The preceding two subsections describe a method that is applicable to optimal control problems, but for which the optimal parameter vector has to be determined. In Ref. 5, an ANN and an EA have been successfully combined to ENC and the applicability of this method as a robust solver for interplanetary low-thrust trajectory optimization problems that needs no initial guess has been demonstrated. Afterwards, ENC was extended by the lead author to planetary low-thrust transfer problems, low-thrust transfers that comprise a change of the central body[9], and flight-phase dependent (staged) propulsion systems. The latter enabled the trajectory analysis for the presented study.

For low-thrust trajectory optimization, ENC works in two nested loops. The inner loop, the trajectory integration loop, uses an ANN to determine the optimal thrust vector direction and magnitude before each integration step. The ANN is called *Neurocontroller* (NC) in this context. Spacecraft state and target state information (position, velocity, fuel) is provided to the NC before every integration step and the NC provides the actual control variables through its output neurons. The next integration step is carried out with the spacecraft state vector and the control variables. As an NC's network function $\mathbf{N}_\pi$ is determined by the network parameter vector $\boldsymbol{\pi}$, one needs to find the optimal parameter vector $\boldsymbol{\pi}^*$ to fly a low-thrust

spacecraft optimally along its trajectory. The NC-parameters are provided by the EA in the outer loop. The genome information of every population member ξ corresponds to a parameter vector $\boldsymbol{\pi}$ and therefore exactly determines one, potentially optimal, solution strategy of the transfer problem. The outer EA-loop, on the other hand, needs an evaluation element to function, and this is implemented through the evaluation of the resulting trajectory at the end of the inner loop. Each solution is assessed w.r.t. to the violation of problem-specific boundary constraints, e.g. final distance to the target in case of fly-by problems and, additionally, the relative velocity in case of rendezvous-type transfers. These constraints are usually user-provided maximum limits. If no limit was violated, the solution is assessed w.r.t. the actual optimization criterion. For low-thrust trajectory optimization problems this is usually either the transfer duration, or the consumed propellant mass, or a combination of both.

D. Spacecraft setup and parameter variation

To carry out trajectory integrations during the optimization runs with *InTrance*, we had to determine the spacecraft configurations for the different propulsion options. This was necessary to obtain values of the problem-determining variables, e.g., the total mass m_0, the propellant mass m_p, and the available maximum thrust in order to configure *InTrance* accordingly. The scientific IHP payload was estimated with $m_{\mathrm{pl}} = 245\,\mathrm{kg}$ for the SEP-only case and with $m_{\mathrm{pl}} = 498\,\mathrm{kg}$ for the SEP+REP-option (including the REP-stage)[8,10]. The SEP-stage was used by all designs; its main components are the structure, the solar power generator with the solar panels, the Xe-filled propellant tank, and the RIT-22 thrust modules.
The solar power generator mass was dependent on its characteristic power P_c, which was defined as the electrical power output at the characteristic distance $r = 1\,\mathrm{AU}$. We chose the unit of percent to express at which power level the SEP-stage could operate at launch, i.e. $P_c = 65\,\%$ allowed the SEP-stage to operate with sixty five percent of maximum available thrust. This proved benficial because it allowed saving of power system and resulting mass. Furthermore, the optimizer was free to explore trajectories with thrust arcs inside Earth orbit, where the spacecraft's full thrust potential could be exploited. Although the trajectory path length thus usually increases, compared to direct transfers, the transfer time can be reduced as acceleration deep in the Sun's gravitiy well is more efficient. We assumed a power-specific mass of 5 kg/kW, which is a realistic assumption when looking at recent developments for deep space mission power generation[11].
InTrance allows the configuration of a user-provided fixed value for the tank mass, or a propellant-mass-dependent one. The latter option requires the provision of the tank mass fraction w.r.t. the propellant mass. A realistic value of this parameter is 0.06.
The thrust modules were of RIT-22-type, an ion engine having been qualified by EADS Astrium Space Transportation. Each of the engines of the propulsion stage was operated at throttle levels between 65 and 100% whereas the NC commanded the actual setting.
The following performance-determining parameters of the propulsion stage were varied to find the configuration that yields the shortest mission duration:

- the number of thrust units, n
- the beam voltage of a RIT-22 thrust unit, U_+, and the resulting specific impulse, I_{sp}
- the electrical power of the solar power generator at 1 AU solar distance, P_c

The SEP-stage contained 4–6 thrust units with beam voltages of 5, 6, or 7 kV. These correspond to an I_{sp} of 7 377, 8 078, and 8 723 s, respectively (see also Table 1). We chose a characteristic electrical power P_c of 65%, 75%, and 85%. The allowed minimal distance to Sun was set to 0.7 AU to prevent thermal problems that might require a special thermal protection system. The REP-stage increased the payload mass for the SEP-stage to 498 kg, and it used a RIT-10-type thruster type with $P = 592\,\mathrm{W}$, (four RTG-based batteries with powerspecific mass of 8.5 W/kg and Begin-Of-Mission (BOM) power of 648 W) $I_{sp} = 3\,810\,\mathrm{s}$, a nominal thrust $F = 21\,\mathrm{mN}$, and a propellant mass flow $\dot{m}_p = 0.558\,\mathrm{mg/s}$. With a RIT-10 lifetime of approx. 23 000 h, four thrust units were necessary to process 158 kg of Xe. The model shown in Fig. 1 and Fig. 2 gives an impression of our IHP spacecraft design with the SEP-stage and the spin-stabilized REP upper stage. We have investigated 54 different spacecraft configurations, being a combination of two different propulsion concepts, three different numbers of thrust units, three different I_{sp}s, and three different solar power generator sizes (as compared to the power that is required by all thrusters at full thrust). These calculations were carried out with C_3=0 (relative to Earth) to assure comparability.

Table 1. Three different RIT22 ion engine characteristics that were used for the *InTrance* runs, whereas the appendices LO, ME, and HI stand for a low, medium, and high I_{sp}-level.

	unit	RIT22LO	RIT22ME	RIT22HI
U_+	kV	5	6	7
I_{sp}	s	7 377	8 078	8 723
F	mN	269	295	319
$\dot{m}_p$	$\frac{mg}{s}$	3.7	3.7	3.7
P	kW	13.59	16.14	18.69

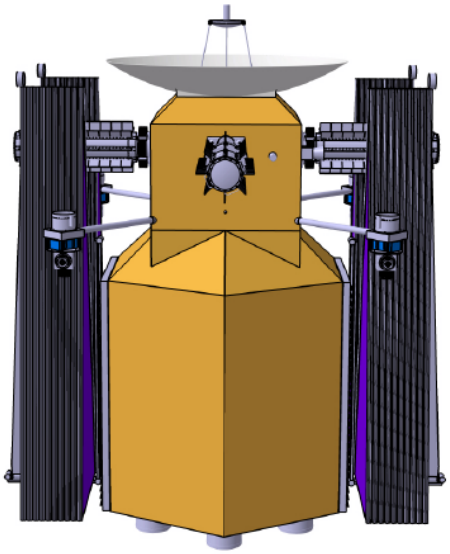

Figure 1. Interstellar Heliopause Probe (IHP) with folded Ultraflex solar power generator panels.

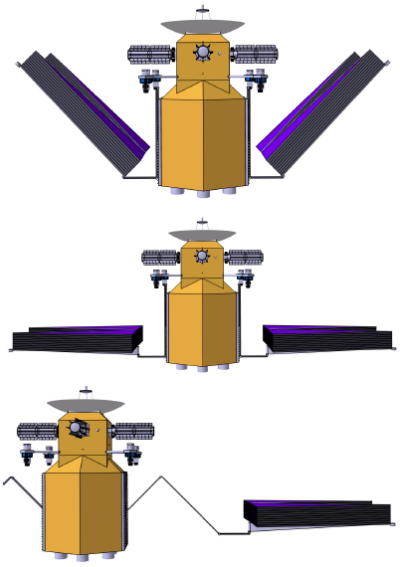

Figure 2. Interstellar Heliopause Probe (IHP) while unfolding its Ultraflex solar power generator panels.

We have used a step-by-step approach, in which we first tried to find the best SEP-only and SEP+REP configuration, i.e. the one with shortest transfer duration, to gain an understanding of the sensitivity to the varied parameters. We identified the number of thrust units, their specific impulse, and the (relative) size of the solar power generator as key spacecraft design parameters. Then we have tried to improve the transfer duration further with a launcher-provided C_3 up to $49\,\mathrm{km}^2/\mathrm{s}^2$. The adaption to the specific launch rocket Ariane 5 ECA together with the optimization of the IHP launch mass was the next step. The final option was the incorporation of a Jupiter gravity assist (JGA). A gravity assist at an outer planet basically can decrease the flight time significantly but at the same time also lower mission flexibility as favorable planet phase angles occur only about once in a decade. This holds especially true if there is a constraint on the direction at which to leave the solar system, e.g. the heliopause's "nose". Due to this disadvantage we have first tried to achieve a flight time of less than 25 years without a JGA.

The SEP-configurations needed only one flight phase, which began at Earth and terminated with the burnout of the SEP-stage, after consumption of whole propellant. During this flight phase, the thrust vector's magnitude and direction was determined by the NC. The SEP+REP-configurations needed an additional flight phase. After burnout and jettison of the SEP-stage, the REP-stage took over. We chose the simple steering strategy "maximum thrust radially away from the Sun" for the second mission phase because the JGA already directs the flight path nearly radially away from the Sun.

III. Results

This section presents the results we have obtained through carrying out multiple *InTrance* optimization runs with different propulsion and power system configurations to find the configuration that yields the fastest transfer to 200 AU solar distance without considering a specific direction.

A. Parameter variation

With a flight time of 28.3 years, the combination of six thrust units with $I_{sp} = 8\,078$ s, a solar power generator with a relative size of 85% (i.e., at 1 AU, it provides 85% of the power that is required to operate all thrust units at full thrust), and a REP upper stage was the fastest out of 54 investigated configurations. Figure 3 shows the flight times and the consumed propellant masses for all 54 configurations.
The utilization of the REP-stage reduced the flight time by 20% in best case and by 10% in worst case and therefore showed the benefit of our double-stage concept on transfer time. However, no configuration was faster than the 25-year limit.
The potentially flight-time-reducing effect of more available electrical power is almost compensated by the increased mass of the necessary bigger solar panels. Within the investigated power range, the size of the power generation subsystem (or the size of its panels) is therefore not a flight-time-sensitive parameter. It has, however, notably influence on technological complexity and resulting cost.
The third investigated parameter, the number of thrust units, however, is more important due to its significant influence on flight time. Figure 3 shows how the usage of an additional unit can account for a flight time saving of up to 3.6 years. The number of thrusters affects technical complexity of the whole spacecraft, its handling, testing, and also cost. Especially if one accounts for mission operations cost and the potential saving of a year of the transfer, this saving may be overcompensated by the cost due to higher technical complexity.
The thrust unit's grid voltage variation showed only minor effect on flight time. The reason is that a higher specific impulse, or the necessary higher acceleration grid voltage U_+, also requires larger solar panels. Due to the resulting mass increase, the thrust gain does not convert to higher acceleration at the same rate. For the following calculations, we have selected the SEP+REP spacecraft with six thrust units, $U_+ = 5$ kV ($I_{sp} = 7\,377$ s), and a solar power generator with $P_c = 65\%$ for reference. The flight time for this reference configuration was 29.6 years. The characteristic power of the solar power generator, i.e. its power at 1 AU, was 53 kW. This value is almost achievable with current technology for geostationary communication satellites, so that our reference configuration IHP design becomes theoretically realizable within the next years. Its transfer time is only 1.3 years higher than the faster but technically more challenging configuration with 28.3 years.

B. Influence of launcher-provided hyperbolic excess energy

The chosen reference IHP-configuration was used for further trajectory optimization calculations with a hyperbolic excess velocity v_∞ between zero and seven kilometers per second. The launch mass m_0 comprised the payload mass, the structure mass, the thrust modules' masses, the propellant mass, and the tank mass, which was set to be 6% of the propellant mass. This allowed *InTrance* not only to minimize the necessary propellant mass, but at the same time to implicitly optimize the required tank mass.

The results in Tab. 2 show a minimum flight time of 27.8 years, which corresponds to a further flight time reduction of 1.8 years, or 6%, but still misses the set 25-year flight time objective by 2.8 years. The propellant mass is 428 kg, a reduction of 37% w.r.t. the reference configuration's propellant mass. Clearly, the influence of additional launch energy on propellant mass is larger than the influence on transfer duration. The positive effect of an increased v_∞ on propellant mass and on flight time becomes smaller with increasing absolute values of v_∞. The largest gain in propellant mass saving and flight time reduction is achieved from 0 km/s to 1 km/s with -21% and -4%, respectively. Further increases of v_∞ up to 6 km/s result in additional 16% propellant saving but only additional 2% in flight time reduction. This potential trade-off between the higher cost for (expensive) Xenon propellant, the higher cost of a maybe necessary high-performance launcher, and the higher mission operations cost due to longer transfer times would be the task of mission designers and is outside the scope of this work.
The v_∞ that a launcher must achieve for the 1 676-kg IHP spacecraft is 6 km/s. Currently existing capable

launch systems, e.g. Delta IV, Atlas V, or Ariane 5, can bring payload masses like this onto interplanetary Earth-escape trajectories, and this was our motivation to adapt the IHP-spacecraft configuration more precisely to the launch characteristics of a specific rocket system.

C. Adaption to the Ariane 5 ECA launch system

Based on our v_∞-variation results, the reference spacecraft configuration was optimized for a launch with the European heavy lift launch system Ariane 5 ECA. This was chosen because it is one of the currently existing launch systems that can provide the required excess velocity of approximately six kilometers per second to a two-ton spacecraft.
The Ariane 5 interplanetary launch performance is available as a plot of C_3 over launch mass m_0 in Ref. 12. For the use within *InTrance*, we have approximated the Ariane 5 ECA launch performance as

$$v_\infty^2(m_0) = C_3(m_0) = \frac{1}{\gamma} \ln\left(\frac{{m_0}^*}{m_0}\right) \tag{2}$$

with a maximum payload mass of ${m_0}^* = 7\,200\,\text{kg}$ for $C_3 = 0$ and a fit parameter of $\gamma = 0.032$ (see also Fig. 4).
Calculations with *InTrance* were conducted the same way as for the v_∞-variation with the C_3-dependent maximum excess velocity now calculated from current launch mass m_0 with Eq. (2). We found the shortest flight time to be 27.5 years and the propellant mass to be 461.2 kg, resulting in a total IHP launch mass of 1 720 kg. The corresponding possible v_∞ was 6.7 km/s and therefore coinciding with what we expected from the results of the v_∞-variation.

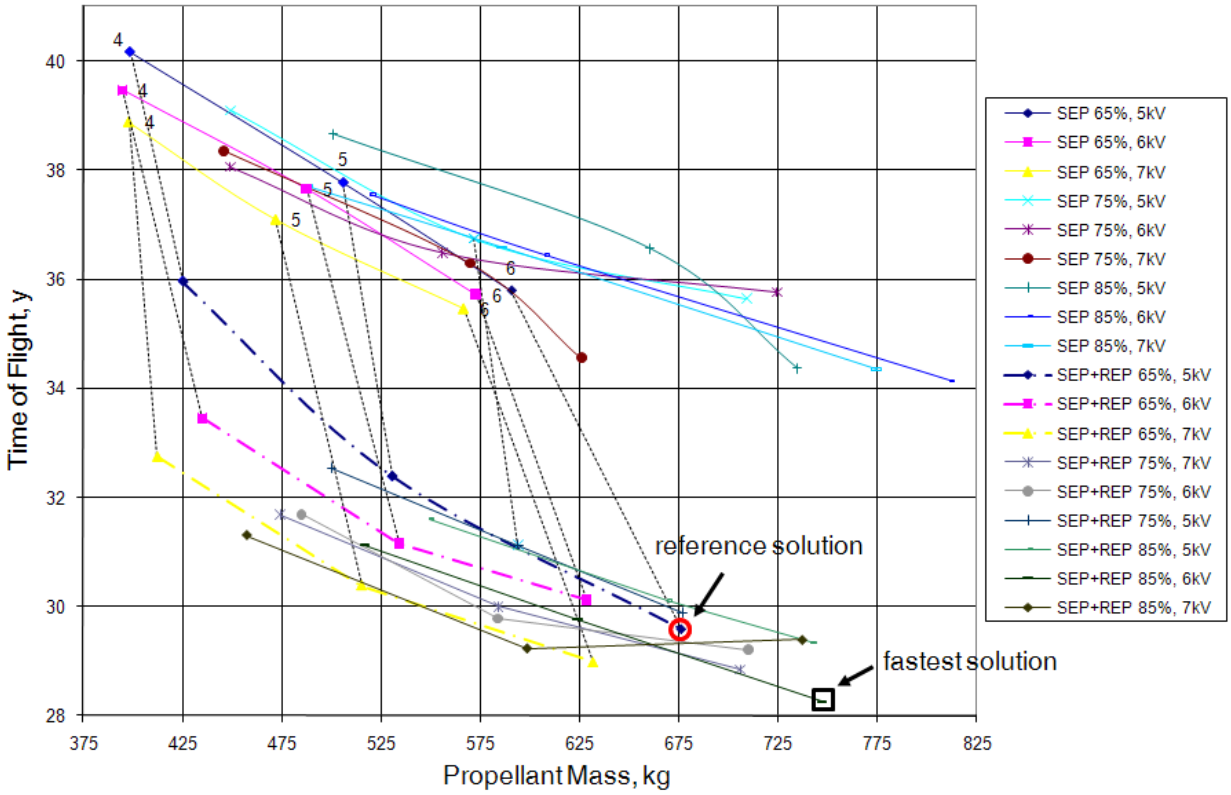

Figure 3. Flight time over propellant mass for 54 IHP spacecraft configurations. For each SEP-only and each SEP+REP design, a different number of thrust units (4, 5, 6), specific impulse of these thrust units (5 kV / 7 377 s, 6 kV / 8 078 s, 7 kV / 8 723 s), and relative solar power generator dimension (65%, 75%, 85%) was set. The fastest solution needs 28.3 years for the transfer, thus being 3.3 years above the limit of 25 years.

Table 2. Propellant mass (m_p), launch mass (m_0), and flight time to 200 AU (Δt) for the reference configuration (six RIT-22 with $I_{sp} = 7\,377$ s and 53 kW solar power generator) with a hyperbolic excess velocity $v_\infty = \sqrt{C_3}$ between 0 and 7 km/s.

v_∞, km/s	m_p, kg	m_0, kg	Δt, yr
0	676	2 095	29.6
1	537 (-21%)	1 821	28.5 (-4%)
2	512 (-24%)	1 787	28.4 (-4%)
3	486 (-28%)	1 753	28.2 (-5%)
4	449 (-34%)	1 703	28.0 (-5%)
5	441 (-35%)	1 693	27.9 (-6%)
6	428 (-37%)	1 676	27.8 (-6%)
7	422 (-38%)	1 668	28.0 (-5%)

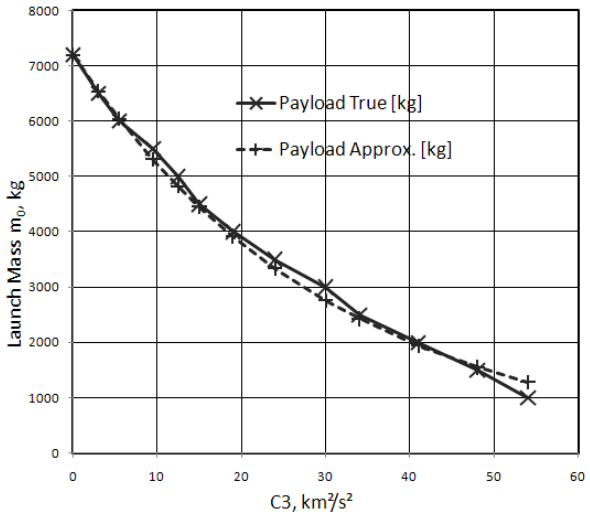

Figure 4. Hyperbolic excess energy C_3 that an Ariane 5 ECA can give to a spacecraft with launch mass m_0. The exact figures from Ref. 12 are approximated with a fit curve according to Eq. (2).

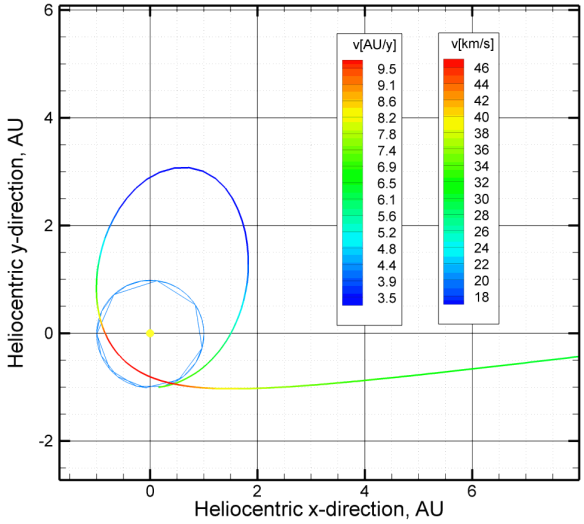

Figure 5. Best solution without gravity assist; launch with Ariane 5 ECA

D. Gravity assist at Jupiter

Including a gravity assist at Jupiter and neglecting the direction of the heliopause "nose" direction finally reduced the flight time to 23.75 years and therefore below the envisaged maximum of 25 years. Table 3 gives the exact figures and Fig. 6 shows the heliocentric trajectory plot. The colored trajectory shows the changing velocity during the transfer. The closeup of the fly-by in Fig. 7 shows how the spacecraft's flight path is bended when passing by behind the planet. The trajectory until encounter of Jupiter includes only a single

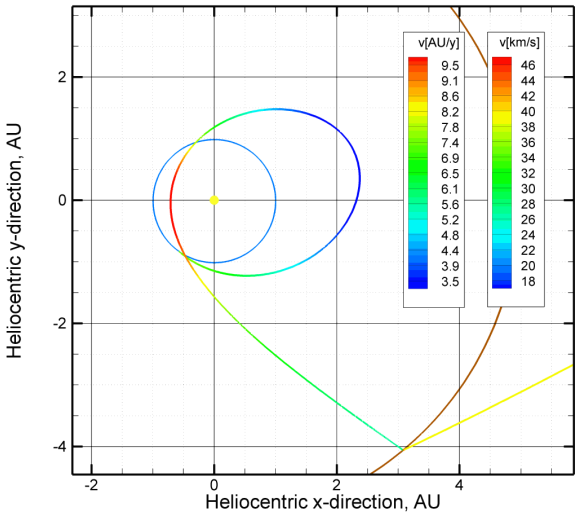

Figure 6. SEP+REP transfer to 200 AU with a gravity assist at Jupiter. The influence of the flyby maneuver, i.e. the increase in heliocentric velocity, is visualized in the abrupt trajectory color change at Jupiter.

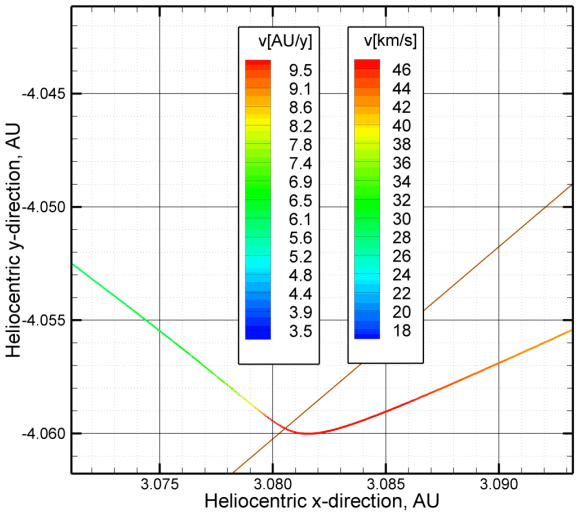

Figure 7. Closeup of the gravity assist at Jupiter. The color coding of the trajectory shows how the spacecraft's velocity is increased when passing by behind Jupiter, whose trajectory is shown in brown.

revolution around the Sun. The adaption to the Ariane 5 ECA launch system provided $C_3 = 45.1\,\mathrm{km^2/s^2}$, which equals a hyperbolic excess velocity of $v_\infty = 6.72\,\mathrm{km/s}$. This launch energy allowed for the immediate increase of the semimajor axis, and therefore the orbit energy, and also the eccentricity of the orbit. Then, while the probe moves towards orbit aphelion, the SEP-thrust is used to lower the perihelion by thrusting in antiflight direction. The perihelion height is now lowered below Earth orbit but not closer than 0.7 AU. Close to perihelion, when the solar panels provide maximum electrical power to the propulsion system, the probe is accelerated with maximum thrust towards Jupiter. The SEP-stage's propellant is depleted after 831 days at a Sun distance of 3.05 AU. When the probe arrives at Jupiter the heliocentric SEP-burnout velocity of 30.5 km/s has reduced to 26.8 km/s due to Sun's gravitation. The close flyby at Jupiter at a distance of only 1.34 Jupiter radii (R_J) results not only in a change of the flight path of approx. 77 degrees, shown in Fig. 7, but also in a change of the heliocentric velocity by $\Delta v = 12.5\,\mathrm{km/s}$.

E. Discussion

Figure 8 summarizes the resulting flight times and propellant masses of our calculations. The four important flight-time-reducing elements are the number of thrust units, the REP-technology upper stage, additional orbit energy through a launch with an Ariane 5 ECA, and the flyby maneuver at Jupiter. The reduced dimensions of the solarelectrical power generator had only minor influence on flight time within the investigated power range but have a positive influence a the mission's technical complexity.

The consequences for mission design of each of the four Δt-relevant elements are however different. Increasing the number of RIT-22 engines also necessitates more propellant, requires a larger tank with higher tank mass, which also leads to a higher structure mass, and consequently increases the launch mass. In our case, the difference in flight time between a SEP-only configuration with four thrust units and the same configuration with six thrusters is 4.4 years and 192 kg of propellant. The corresponding figures for the SEP+REP configuration are 6.4 years and 251 kg.

Table 3. Data of the fastest transfer to 200AU for a SEP+REP configuration and a gravity assist at Jupiter

	unit	value	
Launch date t_l	MJD	58 254.59	(17 May 2018)
m_0	kg	1692	
m_p	kg	440	
C_3	km^2/s^2	45.1	
Δt_{SEP}	d	831	(1.31 yr)
r_{SEP}	AU	3.05	
v_{SEP}	km/s	30.5	(6.44 AU/yr)
v_{J-}	km/s	26.8	(5.65 AU/yr)
v_{J+}	km/s	39.3	(8.29 AU/yr)
d	R_J	1.34	
t_{REP}	MJD	59 225.48	(11 Jan 2021)
Δt_{REP}	d	3.283	(8.98 yr)
r_{REP}	AU	79.60	
v_{REP}	km/s	47.4	(10 AU/yr)
t_f	MJD	66 929.80	(15 Feb 2042)
Δt	d	8 675	(23.8 yr)

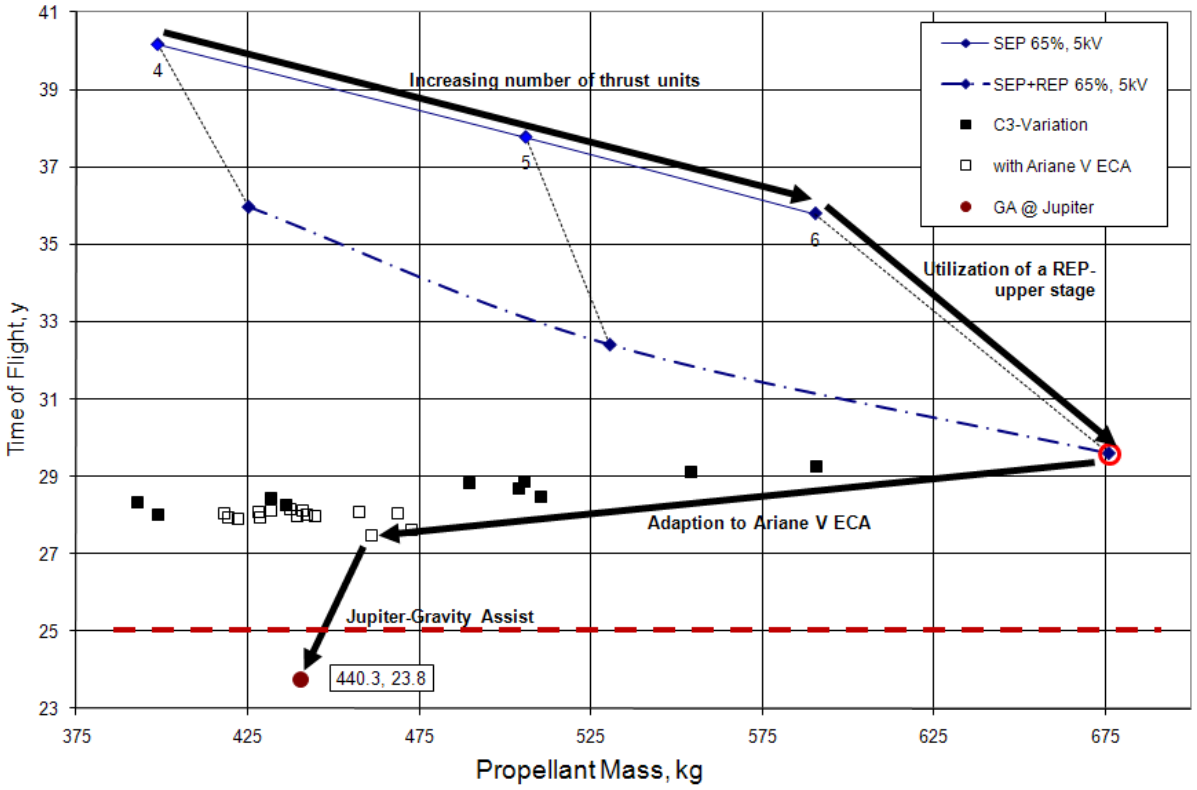

Figure 8. Transfer duration and propellant mass of all investigated configurations. The red circle shows the chosen reference configuration.

IV. Conclusions

Following the flight time limit of 25 years set by ESA for a mission to the heliopause at 200 AU, we have shown that a combination of SEP+REP is a competitive option to solar sailing, which is not yet mature enough for such a mission, and to a combination of electrical and chemical propulsion. However, this was only possible by including a Jupiter gravity assist (JGA). As this particular mission element severely constrains the launch window to a single launch opportunity about every decade, the mission flexibility is significantly reduced. Any mission preparation delay can put the entire mission at risk. That risk is avoidable through a raise of the flight time limit by only 2.5 years. We have shown that with a staged SEP+REP propulsion system and a capable launcher like the Ariane 5 ECA, a flight time of 27.5 years to 200 AU is achievable. This is only 10% longer than the ESA limit and 16% longer than our fastest JGA-solution with 23.8 years. At the same time, this mission concept is more flexible, as it does not need any gravity assist and can therefore launch every year.

Acknowledgments

The support of this work by the German Aerospace Center DLR (project number DLR 50 RS 0901) is gratefully acknowledged.

References

[1]Jaffe, L. J., Ivie, C. V., "Science Aspects of a Mission Beycond the Planets," *Icarus*, Vol. 39, No. 3, 1979, pp. 486-494.

[2]Liewer, P. C., Mewaldt, R. A., Ayon, J. A., Garner, C., Gavit, S., Wallace, R. A., "Interstellar Probe using a Solar Sail: Conceptual Design and Technological Challenges," *The Outer Heliosphere: The Next Frontiers*, edited by K. Scherer, H. Fichtner, H.J. Fahr and E. Marsch, COSPAR Colloquiua Series, 11, Pergamon Press, Amsterdam, 2001, p 411

[3]Lyngvi, A. E., van den Berg, M. L., and Falkner, P., "Study Overview of the Interstellar Helopause Probe," SCI-A/2006/114/IHP, Nordwijk, The Netherlands, 2007

[4]McNutt jr., R. L., Wimmer-Schweingruber, R. F., "Enabling Interstellar Probe," *Acta Astronautica*, Vol. 68, No. 7-8, 2011, pp. 790-801

[5]Dachwald, B., "Low-Thrust Trajectory Optimization and Interplanetary Mission Analysis Using Evolutionary Neurocontrol" Ph.D. Dissertation, Aerospace Dept., University of the Armed Forces Germany, Munich, Germany, 2004.

[6]Dachwald, B., "Optimization of Interplanetary Solar Sailcraft Trajectories Using Evolutionary Neurocontrol," *AIAA Journal of Guidance, Control, and Dynamics*, Vol. 27, No. 1, 2004, pp. 66-72.

[7]Dachwald, B., "Evolutionary Neurocontrol: A Smart Method for Global Optimization of Low-Thrust Trajectories," *AIAA Astrodynamics Specialist Conference*, AIAA-2003-4573, Vol. 1, AIAA, Providence, Rhode Island, 2004, pp. 103-115

[8]Loeb, H. W., Schartner, K.H., Dachwald, B., Ohndorf, A., Seboldt W., "Solar/Radioisotope Electric Propulsion Combination for a Mission to the Heliopause," *32nd International Electric Propulsion Conference*, IEPC-2011-052, Wiesbaden, Germany, Sep. 11-15, 2011

[9]Ohndorf, A., Dachwald, B., Gill, E., "Optimization of Low-Thrust Earth-Moon Transfers Using Evolutionary Neurocontrol," *IEEE Conference on Evolutionary Computation*, CEC-2009-368, Trondheim, Norway, May 18-21, 2009

[10]Loeb, H. W., Schartner, K.H., Dachwald, B., Ohndorf, A., Seboldt W., "Heliopause Probe-SEP Option," German Aerospace Center DLR, DLR 50 RS 0901, Bonn, Germany, 2010

[11]Spence, B., White, S., Wilder, N., Gregory, T., Douglas, M., Takeda, R., Mardesich, N., Peterson, T., Hillard, B., Sharps, P., Fatemi, N., "Next generation ultraflex solar array for NASA's New Millennium Program Space Technology 8," *IEEE Aerospace Conference*, Big Sky, Montana, 2005, pp. 824-836

[12]Ancarola, P., B, "Ariane 5 Performance Optimisation For Interplanetary Missions," *AIAA Astrodynamics Specialist Conference and Exhibit*, AIAA-2002-4902, Monterey, California, Aug. 5-8, 2002